The University of South Bohemia in České Budějovice
Faculty of Science

Researching the capacity of fungal strains to consume methane

Bachelor thesis

Natasha Machate

Supervisor: Dr. Anne Daebeler

Guarantor: Dr. rer. nat Roey Angel

Co-Supervisor: Magdalena Wutkowska, PhD

Consultant: Dr. Rosa P. Calvillo-Medina

České Budějovice 2024

Machate, N., 2024: Researching the capacity of fungal strains to consume methane. Bc. Thesis, in English. − 48 p., Faculty of Science, University of South Bohemia, České Budějovice, Czech Republic.

Annotation

This thesis studies the isolation of fungi from a methane-rich environment, systematically screens them to discern their capacity for methane uptake (as living and dead biomass), and subsequently identifies and characterizes the most promising fungal strains from the samples corresponding with methane uptake.

Keywords

bioremediation, fungal strains, greenhouse gas, methane, methanotrophs, *Trichoderma hazianum*

Declaration

I declare that I am the author of this qualification thesis and that in writing it I have used the sources and literature displayed in the list of used sources only.

České Budějovice, 8th May 2024

……..

Natasha Machate

Acknowledgement

I acknowledge that working on this thesis would not have been possible without the help of those around me who have always supported and assisted me in completing this thesis. Therefore, I sincerely express my deep gratitude to:

1. Dr. Anne Dabeler my supervisor, who was always there to review and made this thesis possible.
2. Magdalena Wutkowska, PhD, my co-supervisor who always took the time to guide me, gave me valuable input and encouraged me to perfect my thesis.
3. Dr. Rosa P. Calvillo-Medina, my consultant who gave valuable suggestions.
4. The Institute of Soil Biology and Biogeochemistry for creating a supportive and friendly environment.
5. All the University Professors who have shared their knowledge with me.
6. My beloved parents who supported me in various ways and always pray for me in all situations.
7. My relatives and friends who have supported me in their ways.

I hope this Bachelor's thesis can provide valuable insights and knowledge for future studies.

Abstract

Several studies have reported the ability of various fungi to consume methane, a greenhouse gas that has a radiative force 28-84 times greater than carbon dioxide, depending on the time frame. However, the available knowledge on fungal methane consumption is inconsistent and sparse. Here, 12 different fungal strains were isolated from methane-rich environments, and five fungi isolated from different media distinct in their nutritional statuses were studied for their putative capacity to uptake methane. The methane uptake was determined for living and dead biomass. This study found that different strains may have capacities to decrease and increase methane concentrations. Different conditions (i.e. growth substrate/media and whether the fungi were alive or dead) resulted in significantly different methane concentration changes. However, this study showed that methane uptake might not always correlate with biomass growth. These findings suggest the need to further study the underlying mechanism of methane assimilation in fungi to understand methane cycling in fungi and to generate effective strategies for reducing methane emissions using fungi.

Contents

1 Introduction

1.1 Global warming and methane

Earth's temperature has increased by approximately 0.06°C per decade since 1850 (del Prado et al., 2023), particularly the year 2023 was the hottest on record (Wong, 2023). The warming of the Earth's temperature aligns with the increase in greenhouse gas (GHG) emissions (Jackson et al., 2020). This GHG emission (i.e. carbon dioxide, methane, nitrous oxide and fluorinated gases) is driven by human activities, according to >99% of scientific peer-reviewed literature (Lynal et al., 2021).

As the second most abundant GHG after carbon dioxide, methane contributes significantly to the greenhouse effect (Montzka et al., 2011). Methane is a trace gas, with two-thirds of emissions produced by anthropogenic processes, for example, in the exploitation of agriculture, farmland and fossil fuels, as a byproduct of organic reactions (Badr et al., 1992; Montzka et al., 2011). Other sources of methane emissions arise from waste treatment (landfills, manure and sewage) and biomass burning (Montzka et al., 2011). Methane is also naturally produced from wetlands, marshes, and methane hydrates due to the anaerobic decomposition of organic compounds in these environments (Badr et al., 1992). According to the U.S. Environmental Protection Agency (2023), methane accounts for almost 16% of total GHG concentration worldwide.

The clear fact is that even though methane is a trace gas with naturally low concentrations, it plays a key role in global warming due to its high global warming potential (Vergara-Fernández et al., 2019). Although methane has contributed less to GHG levels than carbon dioxide, methane is a potent greenhouse gas, with a global warming potential over 20 years (GWP_{20}) of 84 and a global warming potential over 100 years (GWP_{100}) of 28 per unit mass, which means methane is 84 times and 28 times respectively more effective in trapping heat than carbon dioxide in the respective span of years (Jackson et al., 2020; Myhre & Shindell, 2014). Considering the impact of methane on the global climate, it is necessary to prevent methane emissions from as many anthropogenic sources as possible. However, conventional methods, such as flaring, were often costly and problematic. This is because minimal flow rates of 15–30 $m^3\ h^{-1}$ and methane concentrations

preferably above 20–30% *v/v* are required (Lebrero et al., 2016). Also, the flaring method is not possible on pig farms emitting excessive methane because a concentration above 130 g m^{-3} of methane is required for direct combustion (Girard et al., 2012). Methods such as bio covers and soil covers acting as filters have been developed to limit methane emissions, however, a study found that these bio covers can degrade due to the poor material properties of the covers, which in turn can lead to more methane being released into the atmosphere (Sadasivam & Reddy, 2014). Therefore, a cost-effective alternative and innovative method, such as using methane-consuming organisms, is suggested. Methane-consuming organisms have been used for reducing methane in farm odor, landfills, petroleum systems, and coal mines, however, most of them are limited by the hydrophobic nature of methane (Oliver & Schilling, 2016).

1.2 Methanotrophs and monooxygenase

Methanotrophs are microorganisms that oxidize methane as their carbon source to utilize energy in oxic and anoxic environments, producing carbon dioxide as a byproduct (Guerrero-Cruz et al., 2021).

The first methanotrophic bacterium *Methanomonas methanica* was discovered in 1906 (Söhngen, 1906). For a long time, it was thought that only *Pseudomonadota* (Alpha-and Gammaproteobacteria) could aerobically oxidize methane, until 1999, when anaerobic methane oxidizers were described (Figure 1, Hinrichs et al., 1999). Since then, more taxonomic groups capable of oxidizing methane have been discovered over time, such as sulfate-dependent anaerobic methanotrophic archaea (ANME) within the phylum Euryarcaeota, *Methylomirabilis* bacteria, and several species of the *Methanoperedenaceae* family (Figure 1). Over the years, the growth of bacteria on methane has been extensively studied, and the study of only using methane as a substrate was restricted to bacteria and archaea (Wolf & Hanson, 1979; 1980). Notwithstanding the extensive research in prokaryotic organisms, the year 1969 marked the turning point with the first study investigating methane consumption by eukaryotic organisms, particularly yeast in the genus *Graphium* sp., which was found to grow on a mixture of natural gas containing 90.5% methane (Zajic et al., 1969). This impetus spurred other scientists to investigate yeast and fungal strains for their capability to grow on methane. For example, ten years

later, Wolf & Hanson isolated four strains of yeast capable of growing on methane (Wolf & Hanson, 1979).

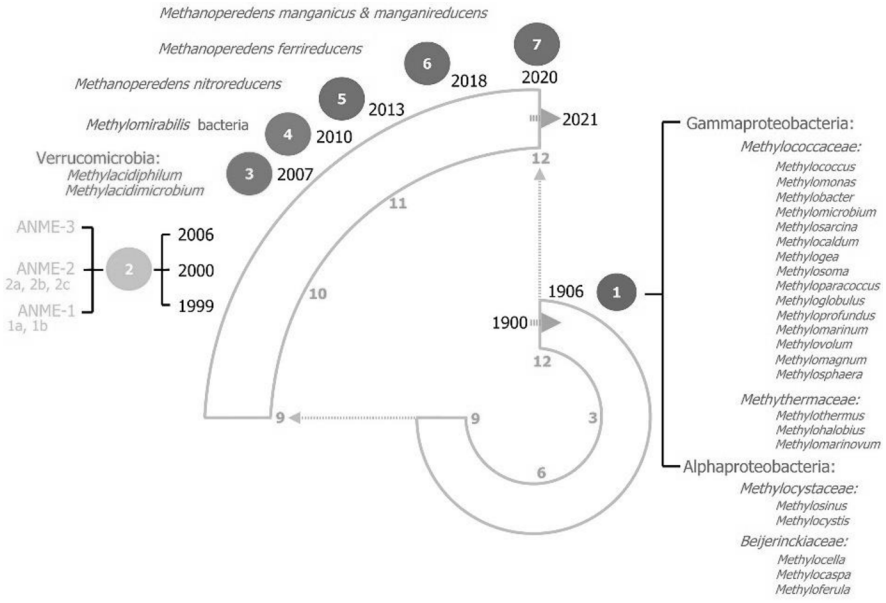

Figure 1. 120 years of discovery of methane oxidizing prokaryotes depicted in a clock-based timeline, each hour on the clock represents one decade (Guerrero-Cruz et al., 2021).

The growth in the presence of methane does not necessarily indicate that these fungi oxidize it; although they are shown to reduce the methane concentration, it has not been confirmed how they are able to reduce methane levels and whether they use it for energy and/or growth (Prenafeta-Boldú et al., 2018). Fungi are not known to encode for any particular or soluble methane monooxygenase enzymes that aerobic methanotrophs use for methane oxidation. However, other enzymes found in fungi are suspected to carry out methane oxidation. One suggestion is the cytochrome P450 monooxygenase, which is universally present in the microsomes of eukaryotic cells for detoxifying harmful chemicals (Prenafeta-Boldú et al., 2018) and has been shown to oxidize gaseous alkanes (Chen et al., 2012; Trippe et al., 2014). Cytochrome P450 monooxygenase was found to be vital in enabling filamentous fungi and yeast to thrive in different environments, as well as n-alkane assimilation. (Črešnar & Petrič, 2011). However, there has been

no conclusive research declaring P450 monooxygenase as the key enzyme for oxidizing methane (Prenafeta-Boldú et al., 2018), nor is there any confirmation about the ability of fungi and yeast to oxidize methane.

1.3 Evidence of methane-capturing organisms

Recent studies by several scientists have identified new genera of yeasts and fungi capable of lowering methane emissions or reducing methane concentration in various environments. For example, in a farm field, Gong et al. showed that *Saccharomyces cerevisiae* could be used to reduce methane production by 25% in pig ruminants, moreover, they were also found to reduce methanogenic archaea in the pig's ruminants (Gong et al., 2013; 2018). Another study conducted by Lebrero et al. (2016) demonstrated the ability of *Graphium* sp. to co-metabolically degrade methane and methanol in a fungal-bacterial biofilter, which enhanced the performance of the previously operated bacterial biofilters (Lebrero et al., 2016). Nonetheless, the capacity of *Graphium* sp. to take up methane alone could not be proved. It was only shown that *Graphium* sp. could reduce methane concentrations when methanol was added (Jensen et al., 1998). On a laboratory scale, Oliver & Schilling found that *Pleurotus ostreatus* had an ability to reduce methane concentrations and observed increasing fungal biomass with concomitantly increased methane capture (Oliver & Schilling, 2016). Interestingly, Liew & Schilling found that not only the live biomass of *Ganoderma lucidum* could reduce methane concentration, but their dried/dead counterparts, too, with an efficiency of 83% in comparison to live biomass (Liew & Schilling, 2020). Although some genera of fungi and yeast have been demonstrated to show their capability to reduce methane levels, there has been very little research to understand what the exact mechanisms are that fungi use for methane capture and how this contributes to the methane cycling in ecosystems.

1.4 Use of fungi in bioremediation

Bioremediation techniques refer to using (micro)organisms to help remove pollutants from the environment (Patel et al., 2022). Using microorganisms for methane abatement is often hindered by poor mass transport and the limited solubility of methane (López et al., 2013).

Despite the fact that the mechanisms through which fungi can capture methane are not known, there are a few studies that have looked at their potential for methane capture. Fungi-based methane bioremediation could potentially be a better biofilter than those based on bacteria as their use increases the effective surface area of the biofilter due to the aerial hyphae that are unique to fungi (Oliver & Schilling, 2016). Furthermore, the reduction of methane levels may be enhanced by cell-surface bound hydrophobins, which decrease the overall hydrophobicity of the fungal surface and improve the sorption of hydrophobic gases such as methane (Lebrero et al., 2016). The study by Liew & Schilling (2020) also showed that fungi increase methane capture by 60-80% compared to purely bacterial biofilters due to their aerial filamentous hyphae, which can extend into the airstream. Another study looking at the efficiency of fungi is the one that was released in 2019 by Vergara-Fernández et al. on the filamentous fungus *Fusarium solani*. They found that *F. solani* speeds up methane degradation in water and reduces the partition coefficient of methane in water by up to two orders of magnitude, thereby increasing methane solubility and capture (Vergara Fernández et al., 2019).

Methane is a potent greenhouse gas; therefore, any research that can propose the understanding of methane cycling in natural systems and bioremediation processes is valuable not only for reducing the amount of methane in the atmosphere but also as an essential contribution to mitigating the climate crisis. This study explores the potential of environmental fungal strains to uptake methane and contributes to methanotrophic research on fungal species diversity.

1.5 Work aims

1. To learn basic microbiological techniques connected with handling and culturing fungi
2. To enrich/isolate fungi from methane-rich environments
3. To screen fungal isolates for their potential to uptake methane
4. To identify and characterize the fungal strains

2 Material and methods

2.1 Sample collection and enrichment of microbial methane consumers

We collected sediment samples into sterile 50 ml tubes from two different locations. The first sample was obtained from a pond in the park Stromovka in České Budějovice, Czechia (48.9672314N, 14.4529306E). The second sample was obtained from a fish pond in Hluboká nad Vltavou, Czechia (49.0414678N, 14.4411369E). These two locations were chosen based on the presence of oxic-anoxic interfaces where methane and oxygen usually overlap.

The collected samples were taken to the lab and placed in separate, sterile 250 ml wide-neck glass bottles and sealed with sterile butyl rubber stoppers and caps on the same day. Methane was added to the headspace to reach a concentration of approx. 10% through injection. Subsequently, the sediment samples were incubated for 10 days in the dark at room temperature. These conditions should favor the development and growth of methane consuming microbial populations.

2.2 Sterilization

1. All of the glassware used in the lab was autoclaved at 120°C for 20 minutes using Classic Prestige Medical autoclave.
2. Butyl rubber stoppers were sterilized in 70% ethanol overnight
3. All the laboratory work was performed in semi- or fully sterile conditions in a UV sterile flowbox (Thermo Scientific™ MSC-Advantage™ Biological Safety Cabinet), using aseptic techniques.

2.3 Solid media preparation

Fungi have diverse nutritional needs. Therefore, we used three media with different nutritional statuses: a nitrate mineral salts medium without carbon sources (NMS; Whittenbury, 1970), Reasoner's 2A medium used for oligotrophic microorganisms (R2A; Reasoner & Geldreich, 1985), and Saboraud-4% Dextrose Agar medium (SDA; Odds, 1991). Depending on the carbon source, these media range from mineral (the least nutrient-rich, with no added carbon source) to the most nutrient-rich for the fungal cells.

The NMS medium, which lacks a carbon source, is routinely used for culturing methanotrophic bacterial microbes (Whittenbury, 1970). To prepare the medium, we followed the NIOO Standard Operating Protocol (NIOO, Netherlands). However, we added only half of the recommended nitrogen source (0.5 g of KNO_3) and added 15 μM lanthanites ($REE_2(CO_3)_3$ x H_2O). To prepare the NMS agar medium, we added the sterile NMS solution to ~4% washed agar to obtain ~1.5% final agar concentration. 1 ml of sterile trace metal solution was added per 1 l of sterile NMS medium (Table 1).

Table 1. Chemical composition of sterile NMS solution per 1 l, dissolved in Milli-Q H_2O.

Chemical	**Amount / a.u.**
KNO_3	0.5000 g
KH_2PO_4	0.5400 g
$MgSO_4$ x $7H_2O$ (9.9824 g in 25 ml Milli-Q H_2O)	1.0000 ml
$CaCl_2$ x H_2O (1.4996 g in 100 ml Milli-Q H_2O)	1.0000 ml
$REE_2(CO_3)_3$ x H_2O	0.0091 g
Trace element solution	1 ml
Trace element solution (amount per liter)	
Na_2EDTA	5.0000 g
$FeSO_4$ x $7H_2O$	2.0000 g
$ZnSO_4$ x $7H_2O$	0.1000 g
$MnCl_2$ x $4H_2O$	0.0300 g
$CoCl_2$ x $6H_2O$	0.2000 g
$CuCl_2$ x $2H_2O$	0.0790 g
$NiCl_2$ x $6H_2O$	0.0200 g
Na_2MoO_4 x $2H_2O$	0.0255 g

For the preparation for R2A and SDA media we used ready-made mixtures. To prepare the medium, we filled a laboratory glass bottle with Milli-Q water and placed a magnetic stirrer in it. Then, we added the respective mixtures according to the manufacturers' instructions. We used 18.13 g l^{-1} for the R2A medium (Himedia, India; SKU M1743) and 65 g l^{-1} for the SDA medium (Merck Millipore, Germany; 105438). Thereafter, the bottles were autoclaved for 25 min at 121 °C by a Classic Prestige Medical autoclave and left at room temperature to cool down. The exact composition for R2A and SDA is depicted in Table 2 and Table 3, respectively.

Table 2. Chemical composition of R2A agar medium in 1 l of Milli-Q H_2O. Final pH (at 25°C) adjusted to 7.2.

Chemical	Amount / g
Casein enzymic hydrolysate	0.250
Peptic digest of animal tissue	0.250
Casein acid hydrolysate	0.500
Yeast extract	0.500
Glucose	0.500
Starch soluble	0.500
K_2HPO_4	0.030
$MgSO_4$ x $7H_2O$	0.500
Sodium pyruvate	0.030
Agar	15.000

Table 3. Chemical composition of SDA agar solution in 1 l of Milli-Q H_2O. Final pH (at 25°C) adjusted to 5.6.

Chemical	Amount / g
Peptone from casein	5.0
Peptone from meat	5.0
D(+) glucose	40.0
Agar-agar	15.0

2.3.1 Preparation of agar plates

After the liquid agar medium cooled down, we added three antibiotics, namely streptomycin sulfate (20 mg ml^{-1}), penicillin G sodium salt (50 mg ml^{-1}) and chloramphenicol (20 mg ml^{-1}). We used these antibiotics to prevent bacterial growth in the culture, as they are abundant in the sediments. Subsequently, the liquid agar medium was poured into sterile plastic Petri dishes inside the flow cabinet and left at room temperature to cool down until solidified. The Petri dishes were

then dried by inverting them. Once the agar had dried, the Petri dishes were closed, placed in plastic bags and stored at 4°C.

2.4 Gradient cell separation

The sediment samples collected at the two sites contained microbial cells and particles, including organic particles, soil, and sediment particles. We carried out the process of gradient cell separation using 80% Nycodenz to separate the heterogeneous particles from the microbial cells (Berry et al., 2003; Morono et al., 2013). In the initial step of the process, 7.0 g of each collected sample was transferred into individual sterile falcon tubes. The next step was to add 25 ml of TN solution (0.2 M NaCl + 50 mM Tris HCl, pH 8.0). The samples were then placed in an orbital shaker at 4°C for 16 h with constant shaking.

At the end of the 16 h shaking period, the sample bottles were transferred to an ice bucket. There, they were subjected to vortex mixing for three cycles, with each cycle lasting 1 min and followed by a 1 min break. Following this mixing step, the samples were centrifuged for 3 min at 700 x g relative centrifugal force (RCF) at 4ºC.

Upon completion of the centrifugation, the supernatant from each sample was decanted into a new 50 ml falcon tube, which was pre-filled with 10 ml of 80% Nycodenz. Then, a second centrifugation cycle was initiated where the falcon tubes were subjected to a second centrifugation for forty minutes at 7197 x g RCF at 4°C. The centrifugation process resulted in the formation of four layers. The microbial layer from each falcon tube was retrieved and transferred into a new 50 ml falcon tube. Subsequently, phosphate buffer-saline (PBS) was added to the microbial layer until a final volume of 35 ml was reached. Then, a third centrifugation cycle was started, which lasted ten minutes at 7197 x g RCF at 4°C. After the centrifugation was completed, the supernatants were carefully removed from the microbial cell pellet that had formed at the bottom of each falcon tube. Then, 1 ml of PBS was added to the microbial cells, followed by a brief vortexing to resuspend them. A portion of the resuspended cells (700 µl) was stored in a cryogenic vial tube filled with 300 µl glycerol, which was kept in a -80ºC freezer for long-term preservation, while the other portion was used for transfer to the plates.

2.4.1 Transfer of isolated cells to respective media

Prior to cell inoculation, the materials and flow box were sterilized using UV light. Then, using a sterile hockey stick, we introduced the cells from each sample by spreading them onto the three different agar media we had prepared previously. This ensured an even distribution of cultures across the respective media.

Finally, we sealed all the plates using semi-permeable tape (parafilm) and stored them inside a 1.5 l GasPak™ system, into which we injected 100% methane to reach approx. 5% methane concentration in the headspace. We incubated this GasPak™ system at 24°C in the dark.

2.5 Fungal strain culturing

In total, 12 random fungal strains with different phenotypes from the three media were selected for cultivation. All procedures involving the handling of fungal strains were conducted under sterile conditions, using aseptic techniques, in a flow box sterilized with UV light and 70% ethanol.

2.5.1 Isolation and transfer of fungal strains

For the filamentous fungi, a sterilized core borer was used to cut a 5 mm disc of agar from a plate with the growing fungus. Prior to each transfer, the core borer was sterilized in 70% ethanol and briefly subjected to flame sterilization. The disc was transferred to a new agar plate with a sterile metal spatula. The agar plate was then sealed with parafilm.

For yeast transfer, we used a plastic loop to transfer each isolate. Using the loop, we picked a single yeast colony and streaked it on the new agar plate. Afterwards, we used parafilm to seal the resulting Petri dish.

2.5.2 Maintenance of fungal isolates

We maintained the twelve fungal isolates on agar plates in a 1.5 l GasPak™ jar with 5% methane in the headspace and incubated them at 24°C. We selected the same environmental parameters throughout the experiment to ensure consistency. Fungi were transferred to new plates to maintain their growth; old plates were kept at 4°C as a backup until the end of the experiment.

2.6 Experimental setup

We selected five isolated fungi because of their rapid growth and coverage of the growth media surface.

Our investigation included both living and dead/inactivated biomass from all the species, as we hypothesized that the dead/inactivated fungal and yeast biomass would exhibit a significant uptake of methane, similar to what has been shown earlier (Liew & Schilling, 2020).

2.6.1 Alive fungi

For the investigation of filamentous fungi, we selected three isolates. We labeled these isolates as F1 (isolated from a SDA plate), F2 and F3 (both isolated from R2A agar plates) (Table 4). To create a sterile environment, we used the procedure described in the previous sections, which involved UV light, 70% ethanol and a flow box. We prepared autoclaved 100 ml laboratory glass bottles for the fungal strains with 25 ml of solid media, 27 bottles in total. We used three different treatments with each three replicates. This way, each fungal isolate was allocated nine bottles (Figure 2).

The setup included the following treatments: fungus incubated in the presence of methane, fungus incubated without methane (untreated controls) and bottles containing agar media in the presence of methane (Figure 2). All treatments were performed with n = 3 replicates, of which three came from the same culture. This setup ensured that we could draw reasonable conclusions from the specimen growth, namely, whether the isolates could uptake methane obligatory or facultatively.

It also helped us differentiate between the methane uptake by the fungi and the media, respectively.

The process involved filling each bottle with 25 ml of appropriate agar media (prepared as previously described) using a serological pipette. After the agar had cooled down, we introduced a drop of the respective liquid media (without agar) into the center of the agar media. We then placed a 25 mm nitrocellulose membrane on top of this drop of liquid media. This membrane would later be used to measure the dry weight of biomass. A drop of liquid media was added on top of the membrane to provide an attachment to the medium for the filamentous fungi to grow. Then, a 5 mm disc of agar from a plate with the growing fungus was transferred onto the membrane. One set of bottles for one filamentous fungus isolate. To seal each glass bottle, butyl rubber stoppers and screw caps were used, and 5 ml of methane from a 100% methane bag was injected into all bottles. They were incubated at 24°C in the dark.

We used liquid media instead of agar media for the yeast experiment to provide the best conditions for the yeast's growth. Before the experiment yeasts were pregrown in liquid media.

We prepared all the liquid media (R2A and SDA liquid media, adhering to the ingredients provided on the powder packaging, but without adding agar). 25 ml of the autoclaved liquid media were transferred into sterile 100 ml glass bottles and inoculated with yeast by loop from the colonies. One set of bottles for one yeast isolate. The bottles were sealed with butyl rubber stoppers, and 5 ml of 100% methane was injected into each bottle. The bottles were then shaken and incubated at 24°C for a week.

After a week, we selected two yeast isolates from seven samples to measure methane uptake. We chose these two isolates based on their rapid growth, which we determined from the liquid media's turbidity and density. The selected isolates were Y1 (isolated from NMS liquid medium) and Y2 (isolated from R2A medium) (Table 4). The setup was similar to the filamentous fungi (Figure 2) but with different amount of media. We added 4.5 ml of the respective media and 0.5 ml of the selected pregrown yeast culture in a 100 ml glass bottle for each isolate. The bottles were sealed, tightened with aluminium crimps and butyl rubber stoppers, and incubated at 24°C in the dark.

Table 4. Fungal isolates that were screened for their capacity to uptake methane. Media type indicate the agar plates from which each isolate was obtained, the same medium was used for cultivation and experiment.

Fungal isolate	Media type
F1	Solid SDA
F2	Solid R2A
F3	Solid R2A
Y1	Liquid NMS
Y2	Liquid R2A

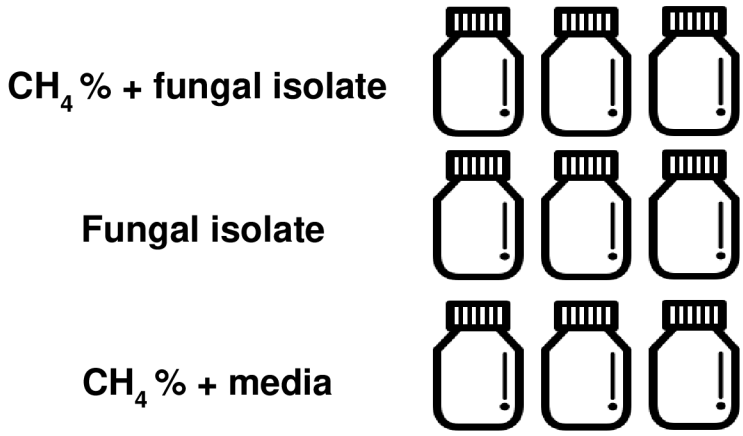

Figure 2. Experimental design to test if isolated fungal strains utilize methane.

2.6.2 Dead/inactivated fungi

Following the completion of the alive fungi experiments, we placed the filamentous fungi in the autoclave at 120°C for 20 min to kill them. Then we transferred them to new sterile 100 ml glass bottles, which we sealed with butyl rubber stoppers and caps. For yeast, all bottles were also autoclaved to kill the cells.

When it was alive, each isolate had two previous treatments: with and without methane. In this experiment, all bottles were sealed and injected with 5 ml of 100% methane. We wanted to investigate the possibility of a difference in methane uptake between dead/inactivated fungi pre-treated with methane when alive and those not pre-treated with methane.

2.7 Methane uptake analysis with gas chromatography

We used a gas chromatograph (Agilent 6850 series) with flame ionization detector (FID) to determine methane concentrations. Using a plastic syringe, gas samples were extracted from each bottle. Injection and oven temperatures were 200^{o}C and 90^{o}C, respectively; head pressure was 34.97 psi with a flow rate of 10 ml min^{-1}. The retention time for each measurement was 4 min. In this setup, we measured methane uptake by the fungus isolates. We extracted 0.1 ml of headspace gas from sealed vials containing the fungi and the growth medium. Additionally, we measured gas samples from vials containing only the growth medium to test whether the medium affected methane concentration (Appendix 2). For filamentous fungi, measurements were taken on the 1st and 7th days of the incubation. For live yeasts, measurements were taken on the 1st, 7th and 14th day. From these data points, we can calculate the mean change in methane headspace concentration as the difference between initial (1st day) and final (7th or 14th day) concentrations, thereby evaluating the capacity of the fungal strains to uptake methane. The gas chromatography (GC) provided the results in the area of the signal produced (pA*s). To obtain the results of the concentration of methane in percentage, we converted the area into concentration (%) by drawing a calibration curve ranging from 0.1% to 5% of methane (Appendix 1). We also subtracted the mean methane concentration change of the triplicates by the mean methane concentration change of their respective media, as the media showed to decrease and increase methane headspace concentration (Appendix 2). We obtained the concentration of 0.1% methane from the methane standard with a concentration of 1000 ppm. Other concentrations were obtained from a 100% methane gas bag, which we diluted to the desired concentrations.

2.8 Biomass analysis

Following the methane uptake analysis, we conducted biomass analysis for each isolate and their untreated control to determine whether there was an increase in biomass corresponding to methane uptake. We used different methods for filamentous fungi and yeast.

2.8.1 Filamentous fungi biomass

For filamentous fungi, we weighed the nitrocellulose membrane with the fungal disc on the 1st day (before measuring methane uptake), and on the 7th day, we measured again the nitrocellulose with the biomass that grew on it. From this, we normalized and calculated the difference between the initial and final weight. On the 7^{th} day, we used sterilized tweezers to remove the nitrocellulose membrane from the bottles that contained the fungal biomass. Each nitrocellulose membrane was wrapped with a pre-weighed piece of aluminium foil. The wrapped membranes were measured using an analytical balance, which provided an accuracy of 0.00001 g for the mass readings.

2.8.2 Yeast biomass

For yeast, we used the optical density of the liquid sample measured at a wavelength of 600 nm (OD600), which measures light scattering through the liquid (Janke et al., 1999). OD600 is used as a proxy for cell density or biomass (Myers et al., 2013); a higher OD600 value indicates a higher concentration of cells (Harnack et al., 1999). The measurements were done using NanoDrop™ One and conducted on fresh well-mixed samples on the 1^{st}, 7^{th}, and 14^{th} days of the experiment. Distilled water was used as a blank sample. A syringe was used for each bottle to sample the yeast culture.

2.9 Fungal strain identification

Fungal strain identification was the last step of our study. We performed Sanger sequencing of the internal transcribed spacer (ITS) region. We first did colony PCR without DNA extraction;

however, the result was unfavourable as no bands were produced. Therefore, our second approach was to first extract the DNA followed by PCR.

2.9.1 DNA extraction

We extracted each strain's DNA using the DNeasy PowerSoil Pro Kit (QIAGEN, Netherlands). The sample was prepared by scraping out the fungi and adding 978 µl sodium phosphate buffer and 122 µl MT lysis buffer. The mixture was then homogenised by centrifugation at 14000 x g for 10 min. The supernatant was transferred to a new tube, and 250 µl PPS was added. The mixture was centrifuged again at 14000 x g for 5 min. The supernatant was transferred to a 15 ml tube, and 1 ml of binding matrix solution was added. The tube was inverted for 3 min. 600 µl of the solution was transferred to a filter tube, where it was centrifuged at 14000 x g for 1 min. Then 500 µl of SEWS-M solution was added to the pellet and centrifuged at 14000 x g for 1 min. The catch tube was emptied, and the pellet was centrifuged again at 14000 x g for 2 min. The DNA was air dried for 5 min, and 100 µl of DES Elution solution was added for centrifugation at 14000 for 1 min. After the DNA was extracted, we performed PCR. We included an extraction control (labeled ctrl) in the PCR reactions besides the positive and negative control, which would show positive in the case of a contaminated kit.

2.9.2 PCR

Initially, we conducted colony PCR, a quicker option, as it did not require extracting DNA from the sample and scraping out colonies directly from each isolate into the master mixes was sufficient. However, standard PCR was a better method for this study based on the results obtained. Even though colony and standard PCR had different sources of DNA, the preparations of master mixes (Table 6), and PCR settings (Table 5) for each were generally the same. We targeted two genes in each fungal isolate. ITS to target and identify fungi and the 16S rRNA to detect if the fungal isolates were contaminated with methane-oxidizing bacteria which could cause the observed methane shifts. As the forward ITS primer we used ITS1catta (5'-ACCWGCGGARGGATCATTA-3') (Tedersoo & Anslan, 2019) and as the reverse primer we used ITS4ngsuni (5'-CCTSCSCTTANTDATATGC-3') (Tedersoo et al., 2014). For the forward

16S rRNA primer, we used 16S-27F (5′-AGAGTTTGATCCTGGCTCAG-3′) (Lane, 1991), and for the reverse primer, we used 16S-1429R(L) (5′-TACGGYTACCTTGTTACGACTT-3′) (Turner et al., 1999). We added two positive controls, referencing samples known to contain a specific gene of filamentous fungi and yeast, and a negative control (PCR grade water), to see if the master mix was not the source of the PCR product. The PCR run time and conditions are depicted in Table 5. We used GeneRuler DNA Ladder Mix (ThermoFischer Scientific, United States) for the ladder.

Table 5. PCR step, temperature, run time, and cycles for ITS and 16S rRNA primer.

Step	**ITS**		**16S rRNA**		**Cycle**
	Temperature	Time	Temperature	Time	
Initial denaturation	95°C	15 min*	94°C	5 min	1x
Denaturation	95°C	45 s	94°C	45 s	
Annealing	48°C	45 s	57°C	30 s	30x
Extension	72°C	1 min	72°C	1 min 15 s	
Final extension	72°C	10 min	72°C	10 min	1x

***15 min:** In standard PCR (ITS), the initial denaturation was 5 min.

We prepared ITS and 16S rRNA master mixes by adding the chemicals shown in Table 6. For the colony PCR, the filamentous fungi biomass was scraped and added to the PCR tube containing the master mix. For each yeast strain, we took a few drops from the bottle and placed them into the PCR tube, using one tube per strain. For the PCR with DNA extraction, 1 µl of the extracted DNA of each strain was added to each tube containing the 24 µl of the PCR master mix.

Table 6. Chemical composition of ITS and 16S rRNA master mix per tube (25 µl).

Chemical	Concentration	Final concentration	Reaction volume/tube (25 µl)
Green Taq buffer	10x	1x	2.5
dNTP Set (Biotechrabbit, BR0600601)	2 mM	0.2 mM	2.5
UltraPure BSA (Thermofisher Scientific, B14)	20 mg ml^{-1}	80 ng μl^{-1}	0.1
Forward primer*	10 µM	0.2 µM	0.7
Reverse primer**	10 µM	0.2 µM	0.7
DNA polymerase***	5 U μl^{-1}	0.625 U	0.13
PCR water			17.4
DNA/template (10ng)			1

***Forward primer:** ITS1catta (ITS), 16S-27F (16S rRNA)
****Reverse primer:** ITS4ngsUni (ITS), 16S-1492R(L) (16S rRNA)
*****DNA polymerase:** For colony PCR DreamTaq™ Hot Start Green DNA Polymerase (ThermoFisher Scientific, EP1712) was used and for standard PCR DreamTaq™ Green DNA Polymerase was used (ThermoFisher Scientific, EP0712)

We prepared the agarose gel to inspect the PCR products by adding 1.5 g of agarose to 100 ml of TAE buffer to reach a 1.5% agarose concentration. The electrophoresis run lasted 30 min at 90 mA. We stained the gel in an ethidium bromide bath for 20 min after the electrophoresis and inspected it in the UV box.

2.9.3 DNA analysis by Sanger sequencing

We washed our PCR products enzymatically using ExoSAP-IT™ reagent according to the manufacturer's instructions. Briefly, we mixed 5 µl of PCR product with 2 µl ExoSAP-IT™ reagent. Then, we incubated them at 37°C for 15 min to degrade the remaining primers and nucleotides, followed by incubation at 80°C for 15 minutes to inactivate the ExoSAP-IT™

reagent. 5 µl of a 5 µM forward primer solution was added to each PCR product. Next, the PCR products were sent for Sanger sequencing (SEQme, Czech Republic). The nucleotide sequences were cut at the beginning and end to remove low quality and overlapping signals. Thereafter, the good-quality fragments were compared to the NCBI standard nucleotide (nr/nt) database using Megablast (Morgulis et al., 2008; Zhang et al., 2000). When compared to the database, the fungal sequence's identity was assigned based on the best score, identity, and e-value.

2.10 Statistical analysis

To test the significant reduction in methane concentration and biomass growth of each fungal isolates, statistical analyses were performed using R 4.2.2 (RStudio Team, 2022). Normal distributions were tested using the Shapiro-Wilk normality test ($p > 0.05$). A respective statistical test was then implemented to validate the result obtained. To confirm the significant change in methane concentration, and biomass growth relative to the starting measurement value, a paired t-test ($p < 0.05$) was conducted separately for each isolate, along with their untreated controls. A t-test ($p < 0.05$) was performed for each isolate to see if there were differences between methane pre-treated and not pre-treated in the dead fungal biomass and a one-way analysis of variance (ANOVA) with a post-hoc comparisons test (Tukey's HSD; $p < 0.05$) was used to compare the significant difference in the methane concentration change compared to their living biomass. Pearson's correlation ($p < 0.05$) was conducted to confirm the relationship between biomass growth and methane concentration change.

3 Results

3.1 Fungal strains

We isolated 12 fungal strains (Figure 3). Five strains that grew the fastest with methane in their headspace were chosen for further examination. Among them, three were filamentous (F1, F2,

and F3), and two were yeast (Y1 and Y2). F1 was isolated on SDA medium, forming white-yellow filaments that thoroughly covered the plate. F2, producing white filaments and green conidia was isolated on R2A medium. F3 was also isolated in R2A medium and grew in white filaments that were thinner than those of F1. Y1 was isolated on NMS medium, and had flat transparent colonies. Y2, which was isolated on NMS medium, had flat, beige colonies.

We assigned their taxonomy based on the result of the ITS sequence alignment comparison with the existing DNA database (Table 7). During the study, Y1 was assumed to be a yeast, however, the PCR results showed a band in the 16S rRNA gene and no PCR product for the ITS (Figure 4). The Sanger sequence of the 16S rRNA gene showed the highest similarity to *Pseudomonas migulae*, with a putative multidrug antibiotic-resistance, as it grew with the addition of three antibiotics. For all of the other fungal isolates we did not obtain any 16S rRNA gene products visible in the gel, but for all of them there was one clear band visible for ITS. Y2 ITS showed three similar %identical alignment results with *Pichia* sp., *Saccharomycete* sp. and *Saturnispora silvae.* With *Pichia* sp. and *Saccharomycete* sp. Y2 was 100% identical, whereas with *S. silvae,* it was only 99.58%.

Filamentous fungi F1, F2, and F3 looked differently when growing on plates with SDA and R2A medium (Figure 3). Based on these phenotypic differences, we assumed that they were different species. However, the ITS taxonomy annotated the three isolates as the same species, *Trichoderma hazianum*. They had different e-values and max. scores. Nevertheless, they were 100% identical for all three strains.

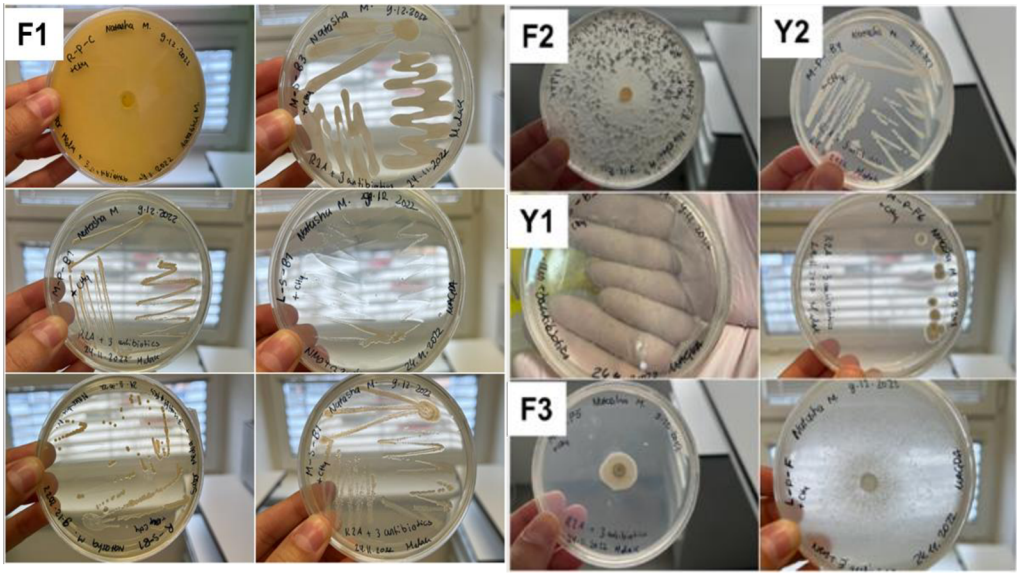

Figure 3. Fungal isolates obtained in this study. From the 12 isolates, five were chosen to test methane utilization, labeled F1 (SDA medium), F2 (R2A medium), F3 (R2A medium) for filamentous fungi and Y1 (NMS medium), and Y2 (R2A medium) for yeast.

Table 7. DNA analysis result for Y1, Y2, F1, F2 and F3, including its length, start sequence, end sequence, scientific name, max score, query cover, e-value, % identical and accession length.

Isolate initial	Marker length	Start sequence*	End sequence**	Scientific name	Max score	Query cover	E-value	% identical	Accession length
Y1	1120	89	882	*Pseudomonas migulae*	1465	100%	0.0	100.00	1440
				Pichia sp.	436	100%	$7.00 \cdot 10^{-118}$	100.00	566
Y2	400	91	327	*Saccharomycete* sp.	436	100%	$7.00 \cdot 10^{-118}$	100.00	367
				Saturnispora silvae	431	100%	$3.00 \cdot 10^{-116}$	99.58	479
F1	580	131	368	*Trichoderma hazianum*	438	100%	$2.00 \cdot 10^{-118}$	100.00	645
F2	570	29	460	*Trichoderma hazianum*	797	100%	0.0	100.00	645
F3	580	121	366	*Trichoderma hazianum*	453	100%	$7.00 \cdot 10^{-123}$	100.00	645

***Start sequence:** The point where the good sequence begins after removing low-quality sequence from the beginning.

****End sequence:** The point where the good sequence ends after removing low-quality sequence from the end.

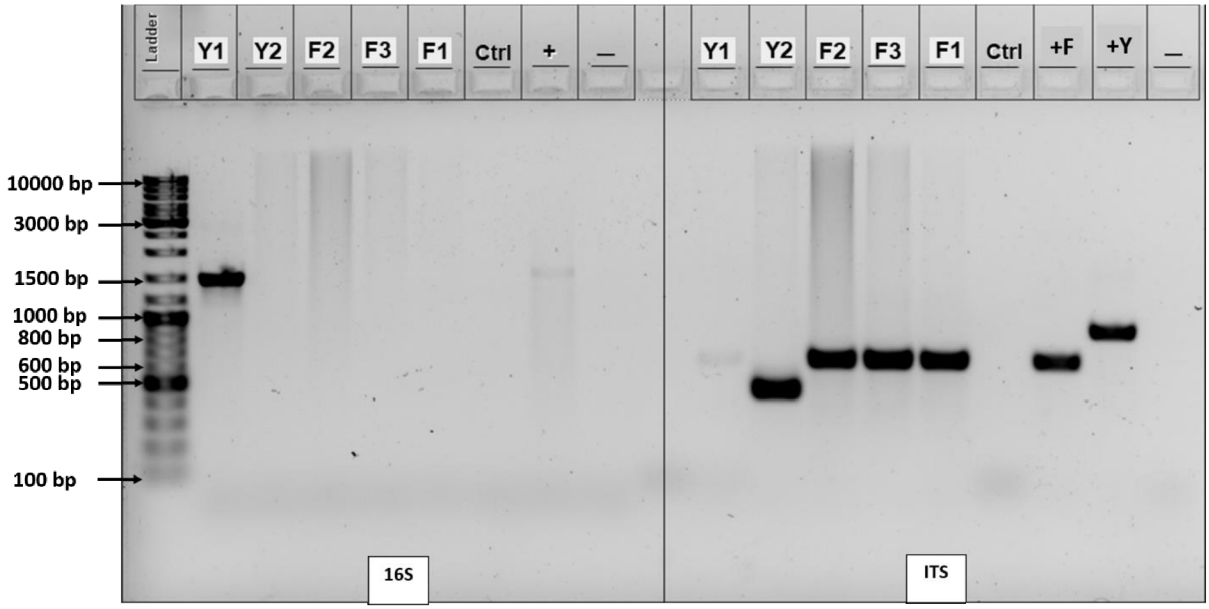

Figure 4. Screening PCR products. Left side consisted of 16S rRNA products, a control for the DNA extraction kit (ctrl), positive control (+) and negative control (-). Right side consisted of ITS products, a control for the DNA extraction kit (ctrl), positive control filamentous fungi (+F), positive control yeast (+Y) and negative control (-).

3.2 Methane uptake capacity

Screening the methane headspace concentration differences between the beginning and end of the experiments allowed us to analyze the methane uptake capacity of the five fungal isolates.

3.2.1 Methane uptake capacity of alive fungi

Relative to their initial methane headspace concentration, two of the tested filamentous fungi (F2 and F3) did not significantly change their methane headspace concentration after one week of incubation (Table 8). Unlike the two filamentous fungi, F1 significantly decreased methane headspace concentration and notably had the highest reduction in methane headspace concentration, up to 35%. The pattern was consistent among the three replicates of F1 (Figure 5a). In contrast, one of the replicates of F2 and F3 had inconsistent trends in methane changes (Figure 5b and c), resulting in a high standard deviation (Table 8). For instance, the methane concentration

of replicate F3A increased instead of decreasing as in the other two replicates. In comparison, F2 had a higher change in methane headspace concentration, which was 12.7 percentage units different than F3. Both F2 and F3 were grown in solid R2A media, in which the solid R2A medium control was observed to cause a decrease in methane headspace concentration of 10% (Appendix 2). In contrast to the filamentous fungi, both Y1 and Y2 had significant increases in methane headspace concentrations of up to 16% and 14%, respectively. For Y1, the highest rise was observed during the first week of incubation, followed by a slight increase in the second week (Figure 5d). Meanwhile, Y2 showed a prominent rise in the second week (Figure 5e).

Table 8. Means (±standard deviation) of initial, and final methane headspace (%) and means (±standard deviation) of change in methane headspace (%) of five tested living fungal isolates (n=3 per isolate). Negative and positive value of the mean change in methane headspace indicate methane (%) decrease and increase respectively. The p-value of the paired t-test between initial and final methane headspace (%) is presented with *significant at $p<0.05$.

Isolate	Initial methane headspace (%; Mean ± S.D.)	Final methane headspace (%; Mean ± S.D.)	Change in methane headspace (%; Mean ± S.D.)	p-value
F1	3.62 ± 0.38	2.21 ± 0.25	-34.64 ± 4.63	0.017*
F2	3.85 ± 0.27	3.05 ± 1.01	-13.30 ± 24.38	0.327
F3	4.02 ± 0.34	3.67 ± 0.25	-0.60 ± 14.34	0.483
Y1	4.51 ± 0.15	5.14 ± 0.23	+15.84 ± 2.69	0.009*
Y2	5.31 ± 0.08	5.76 ± 0.14	+13.88 ± 1.53	0.037*

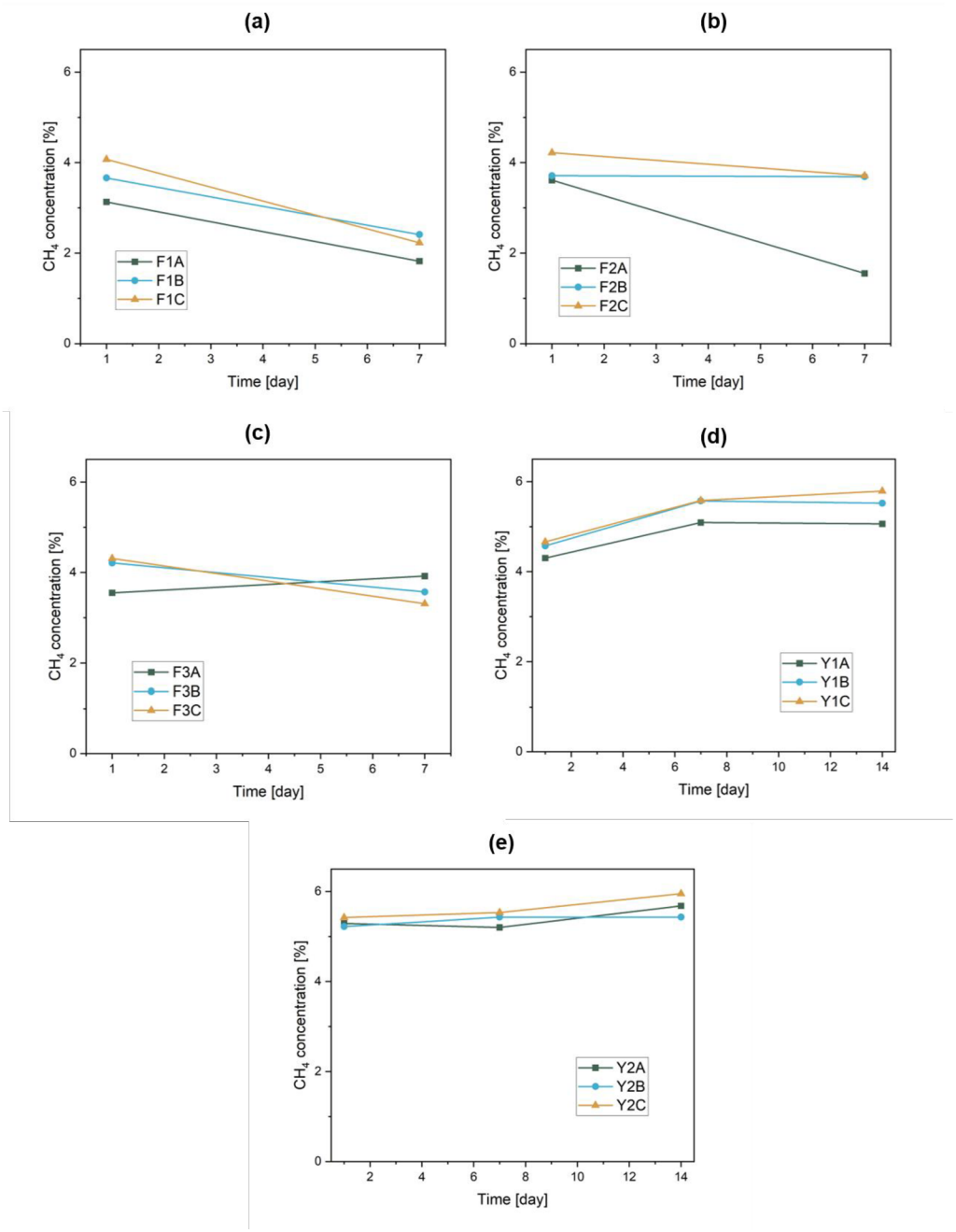

Figure 5. Changes in methane headspace concentration (%) during the experiment testing fungal living biomass. **(a)** F1, **(b)** F2, **(c)** F3, **(d)** Y1, **(e)** Y2. The points on day 1 represent the initial methane headspace concentration and the points on day 7, and 14, respectively, represents the final methane headspace concentration after incubation. The different color lines represent replicates (A, B, C).

3.2.2 Methane uptake capacity of dead/inactivated fungi

We tested the dead/inactivated fungi isolates to see if they uptake more methane than their live counterparts, as observed in a previous study (Liew & Schilling, 2020). The t-test revealed no statistically significant effect of pre-treatment with methane on the change in methane headspace ($p > 0.05$). As a result we can deduce that, only the isolates are responsible for the change in methane headspace concentration. Interestingly, all the fungal isolates behaved differently than in their live experiment; mainly, F1, Y1, and Y2 had significant differences in the change in methane headspace concentration compared to their living biomass based on the one-way ANOVA and Tukey's HSD test ($p < 0.05$). In this experiment, F1 did not show a reduction in methane headspace concentration compared to the live experiment, which was revealed to reduce 35% of the injected methane concentration. In fact, instead of decreasing, methane headspace increased by 11-15% (Table 9). Unlike the live experiment, F3 was also shown to increase methane levels in the headspace up to 16%, although there was an inconsistency between the replicates (Figure 6c). Generally, F2 showed a slight change in methane headspace concentration by 1% with differences in pre-treated and non-pre-treated conditions by means of decrease and increase, respectively (Table 9). Strikingly, Y1 showed a significant reduction in methane headspace concentration by up to 19%, contrary to their living biomass, where it increased significantly. Y2 was also shown to increase methane concentration in this experiment, and there was a significantly lower increase in methane headspace concentration compared to their living biomass (Table 9). Generally, all replicates had fairly consistent values (Figure 6).

Table 9. Means (±standard deviation) of initial and final methane headspace (%) and means (±standard deviation) of change in methane headspace (%) of five tested dead/inactivated fungal isolates (n=3 per isolate) with two conditions: 't' represents isolate that had been pre-treated with methane when alive and 'nt' represents isolate that had not been pre-treated with methane when alive. The p-value of the paired t-test between initial and final methane headspace (%) is presented with *significant at $p<0.05$. Superscript 'a' on the change in methane headspace column represents significant difference ($p<0.05$, one-way ANOVA and Tukey's HSD) in the change of methane headspace concentration compared to the living biomass.

Isolate	Condition	Initial methane headspace (%; Mean ± S.D.)	Final methane headspace (%; Mean ± S.D.)	Change in methane headspace (%; Mean ± S.D.)	p-value
F1	t	3.32 ± 0.22	3.65 ± 0.09	+14.72 ± 11.52 [a]	0.229
	nt	3.31 ± 0.13	3.54 ± 0.21	+11.04 ± 9.97 [a]	0.357
F2	t	3.49 ± 0.15	3.18 ± 0.47	-1.24 ± 9.79	0.239
	nt	3.43 ± 0.14	3.21 ± 0.42	+1.10 ± 9.11	0.325
F3	t	3.08 ± 0.15	3.16 ± 0.17	+10.05 ± 3.34	0.318
	nt	3.33 ± 0.37	3.58 ± 0.28	+16.16 ± 14.81	0.479
Y1	t	4.42 ± 0.10	3.55 ± 0.22	-18.75 ± 3.12 [a]	0.007*
	nt	4.45 ± 0.40	3.78 ± 0.19	-13.72 ± 6.44 [a]	0.062
Y2	t	4.69 ± 0.09	4.79 ± 0.09	+2.09 ± 1.00 [a]	0.064
	nt	4.52 ± 0.20	4.70 ± 0.22	+3.50 ± 1.89 [a]	0.070

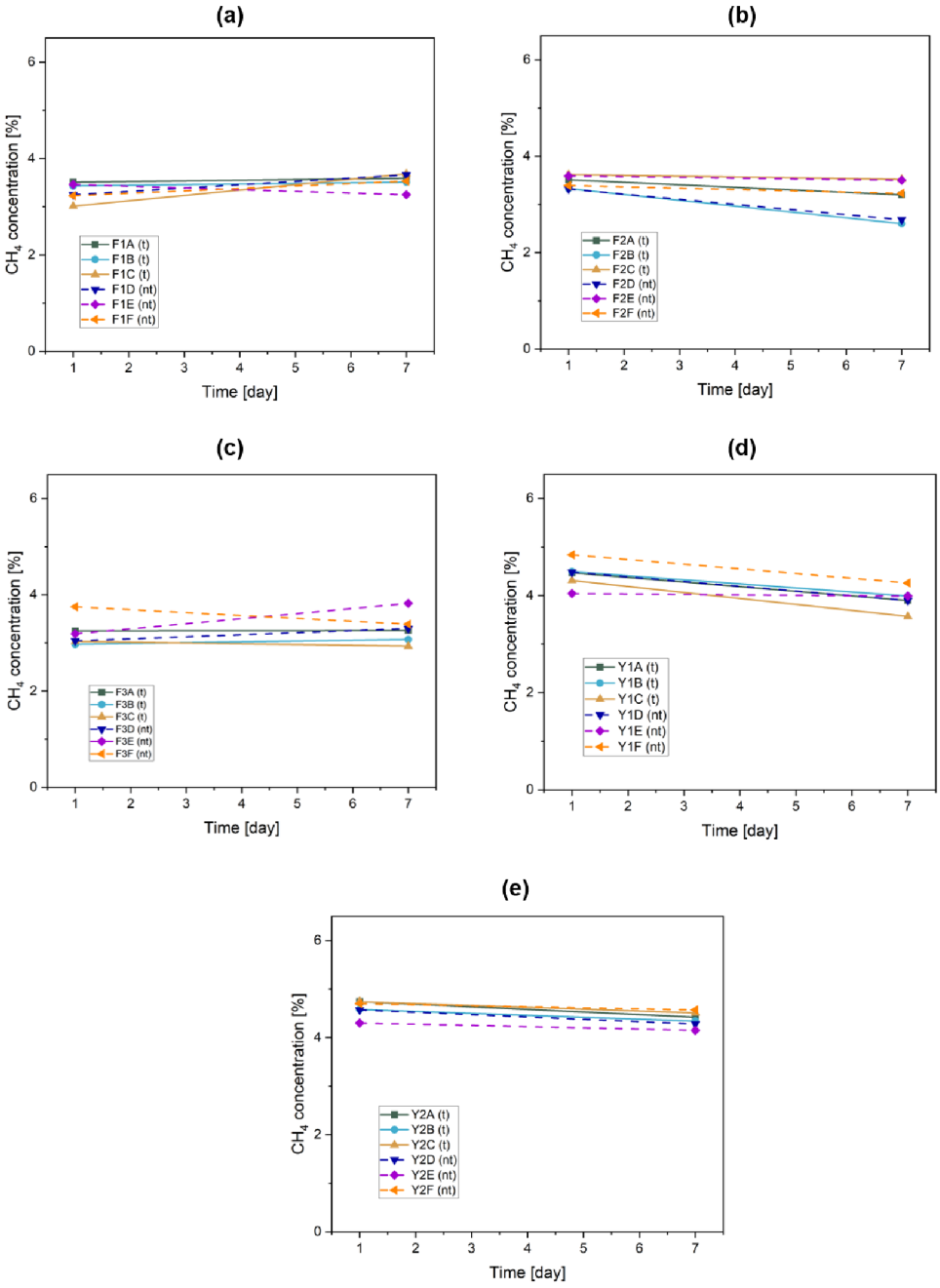

Figure 6. Changes in methane headspace concentration (%) during the experiment testing fungal dead/inactivated biomass. **(a)** F1, **(b)** F2, **(c)** F3, **(d)** Y1, **(e)** Y2. The points on day 1 represent the initial methane headspace concentration, and the points on day 7 represent the final methane headspace concentration after one week of incubation for each of the replicates. The different color lines represent replicates (pre-treated: A, B, C; untreated: D, E, F). The solid lines correspond to isolates that have been pre-treated with 5% methane (t) in the alive experiment and the dashed lines to those that have not been pre-treated (nt).

3.3 Biomass of fungal strains

In this sub-section, we present the biomass results produced by the five living fungi. This measurement is used to observe the relationship between methane uptake and biomass production. The three filamentous fungi with two conditions (methane treated and untreated) did not grow significantly based on the paired t-test value ($p > 0.05$). Out of the three isolates, F1 showed the highest biomass growth when treated with methane 0.097 g, and when not treated with methane, it had the lowest biomass compared to F2 and F3 (Table 10). In contrast, F2 had lower biomass growth when treated with methane by 0.062 and 0.082 g, compared to F3 and F1 respectively (Table 10) and showed the lowest increase profile (Figure 7b). Although there were no significant correlations between methane uptake and biomass growth, as confirmed by Pearson's correlation test ($p < 0.05$), the three isolates showed different trends. For F1, a strong positive correlation ($r = 0.971$) was obtained. For F3, a moderately positive correlation ($r = 0.417$) was observed, and for F2, a negative correlation ($r = -0.684$) was observed. Notably, the difference in biomass growth between different conditions (i.e. treated with methane and untreated) was significant, as confirmed by the t-test ($p = 0.018$), and the isolates treated with methane (straight lines) had a significantly higher slope, which corresponded to more biomass growth when treated with methane (Figure 7).

Table 10. Biomass growth of filamentous fungi during the experiment testing fungal living biomass treated with methane and untreated. $+CH_4$ represents fungi treated with methane and '– 'represents untreated fungi controls. Means (±standard deviation) of biomass growth (g) by three filamentous fungi isolates (n=3, per isolate), measured from the initial and final weight.

Isolate	Condition	Biomass growth (g; Mean ± S.D.)
F1	+ CH_4	0.097 ± 0.064
	–	0.006 ± 0.005
F2	+ CH_4	0.015 ± 0.020
	–	0.007 ± 0.006
F3	+ CH_4	0.077 ± 0.053
	–	0.007 ± 0.006

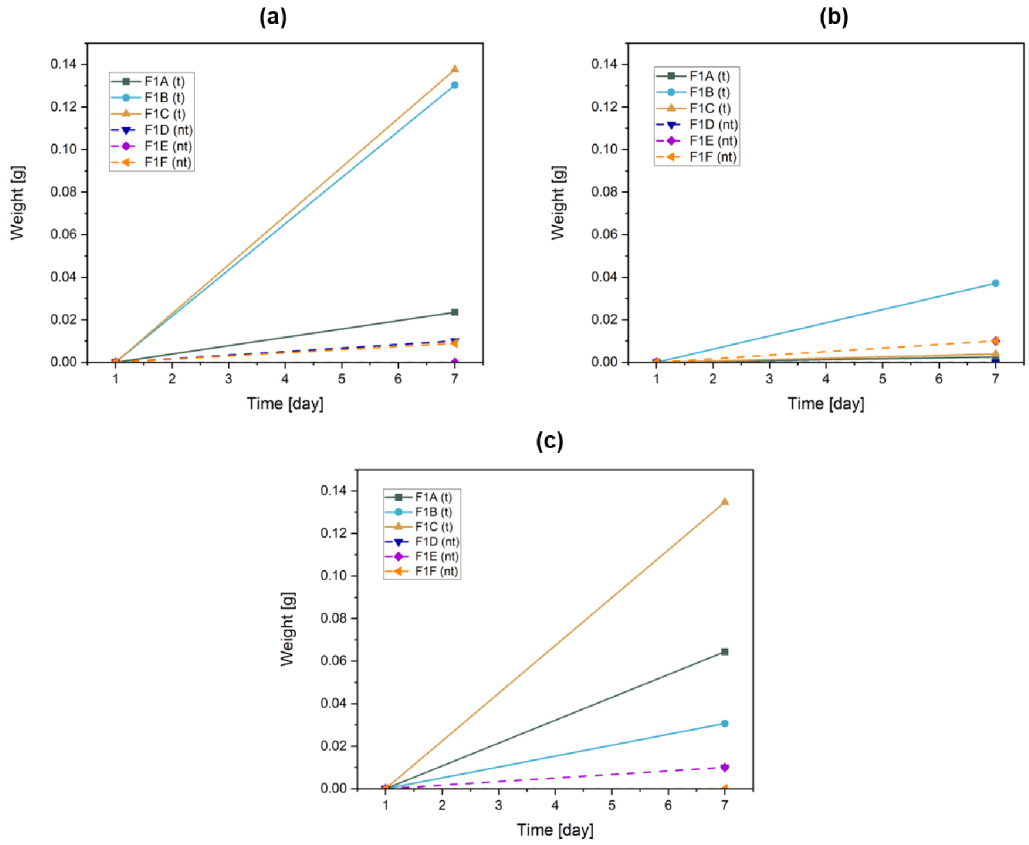

Figure 7. Biomass growth (g) during the experiment testing fungal living biomass treated with methane (solid lines) and untreated (dashed lines). **(a)** F1, **(b)** F2, **(c)** F3. The lines from day 1 to day 7 represent the normalized weight (g) initially and after one week of incubation, respectively. The different color lines represent the replicates (treated with methane: A, B, C; and untreated: D, E, F).

Notably, the OD600 measurement of the cell growth showed that both yeast isolates increased significantly relative to the initial cell density, as confirmed by t-test ($p < 0.05$) (Table 11). In this case, Y2 had a 2x more increase in cell density than Y1 for both conditions (Table 11), although it increased methane levels in the headspace less than Y1. The t-test showed no significant difference in the cell density between isolates treated with methane and those untreated ($p > 0.05$). However, for Y1, the untreated isolates were 0.197 units higher, and for Y2, the treated ones were 0.08 units higher. Nevertheless, these differences were not significant ($p > 0.05$). The three replicates of each isolate showed a consistent increase, and the first week of incubation with methane appeared to be the time when the cells grew the most shown by their steep slopes (Figure 8). After the second week of incubation, the cells' growth began to slow down (Figure 8). Pearson's correlation test was conducted for the two yeasts to determine if there was a correlation

between the change in methane headspace and cell growth. For Y1, the correlation test showed a positive relationship (r = 0.88) and for Y2 a negative relationship was observed (r = -0.61). For both of the relationships, the correlation was not significant ($p < 0.05$).

Table 11. Cell growth of living yeast isolates during the experiment. Means (±standard deviation) of growth in cell density (OD600) by two yeast isolates (n=3, per isolate) relative to the initial OD600 value. '+CH_4' represents yeasts that have been treated with methane and '–' represents yeast controls that were untreated. '*' represents significant growth (paired t-test $p<0.05$) between initial and final OD600 value.

Isolate	Condition	Biomass growth (OD600; Mean ± S.D.)
Y1	+CH_4	0.360 ± 0.017*
	–	0.557 ± 0.200*
Y2	+CH_4	2.723 ± 0.206*
	–	2.643 ± 0.151*

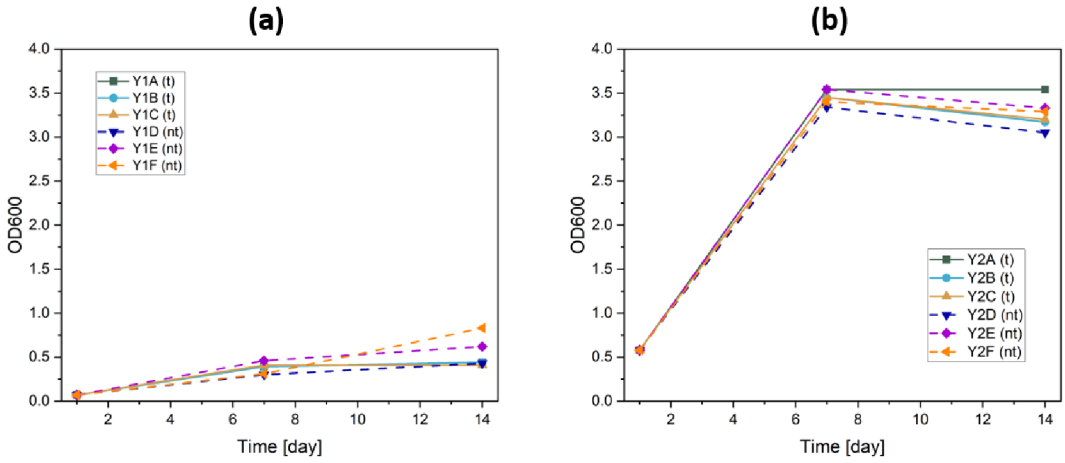

Figure 8. Cell density growth measured through OD600 during the experiment testing yeast living biomass treated with methane (solid lines) and untreated (dashed lines). **(a)** Y1, **(b)** Y2. The points on day 1 represent the OD600 value initially. The points at day 7 and 14 represent the OD600 values after one and two weeks of incubation. The different color lines represent the replicates (treated with methane: A, B, C; and untreated: D, E, F).

4 Discussion

Among the five fungal isolates, F1 demonstrated a significant capacity to reduce methane headspace concentrations up to 35% relative to the starting concentration (Table 8). Despite identical taxonomic assignments (Table 7), F2 and F3 displayed approximately three times lower reduction in methane concentration (Table 8). Additionally, the biomass analysis showed that there was a positive correlation between the methane uptake of F1 and its biomass growth; this may indicate that the growth is partly due to methane consumption, as Oliver and Schilling reported that the ability to uptake methane generally increases fungal biomass (Oliver & Schilling, 2016; 2018). Studies have also reported that the genus *Trichoderma* grew in fuel tanks, assimilating n-alkanes (Prenafeta-Boldú et al., 2018). Moreover, the cell growth was significantly higher when treated with methane than the untreated controls (Table 10). Although a positive correlation was confirmed, and the studies mentioned reported a correlation between methane uptake and biomass growth, the biomass increase in F1 was not significant ($p > 0.05$). For F3, a positive correlation was also observed, even though F3 did not significantly reduce methane. In contrast, the biomass growth of F2 was negatively correlated, meaning that with less reduction in methane level, the cells grew more. This observation did not align with the study that mentioned the correlation between biomass growth and methane uptake in different fungal strains (Oliver & Schilling, 2016; 2018). This could imply that methane might not play a role in fungal carbon fuel for all methane-capturing fungi. Therefore, more studies with more replicates need to be conducted to understand methane capture and possible assimilation in *T. hazianum* and its capacity to reduce methane emissions.

In our observation, the fungal isolates F2 and F3 were shown to have different methane uptake capacity (Table 8) and physical features (i.e. shape and colour) (Figure 3) than F1, even though their ITS fragments were all most similar to *T. hazianum* (Table 7). This variability in methane uptake capacities and physical structures may be explained by differences in metabolite production reported in several studies. For example, studies by VanderMolen et al. (2013) and Adelusi et al. (2022) have shown that even genetically identical fungi can produce different metabolites when grown under different growth substrates (Adeulsi et al., 2022; VanderMolen et al., 2013). Furthermore, *Trichoderma* spp. are usually found to possess an atypical hyphal size,

and when grown on different growth substrates (i.e., standard carbohydrate media), they begin to develop typical conidiophores and conidia (Zajic et al., 1969), as observed in F2, and F3 (Figure 3). In this experiment, the difference was due to the media/growth substrate: F1 was grown in SDA, which consisted of a high amount of variety of carbon sources, and F2 and F3 were grown in R2A, which had fewer carbon sources than SDA (Table 4). Thus, the difference in methane headspace concentration reduction could be attributed to the distinct metabolites each strain produces in response to its specific growth medium. Moreover, R2A medium was found to uptake methane up to 10%, nearly the amount of F2 and F3 in reducing methane concentration (Table 8); thus, the methane concentration reduction of F2 and F3 could also be due to the medium and not solely carried out by the fungi. A similar methane uptake by malt agar medium of up to 26% was also observed in the experiment of Liew and Schilling (Liew & Schilling, 2020). Overall, the substrates in the growth media likely play a role in determining fungal morphology and metabolite production, thereby influencing their capacity to capture methane. Moreover, certain media may lead to methane capture abiotically.

Another possibility for these observed differences in behaviour between F1, F2 and F3 with the same taxonomically assigned strain, *T. hazianum*, is that using one marker (one gene) to distinguish species was possibly not sufficient, and some groups require several markers to find out the differences. Fischer and Gillis suggested that more than one marker is needed to identify unknown cells (Fischer & Gillis, 2021).

Interestingly, Y1 and Y2 did not reduce methane in the live experiment but instead significantly ($p < 0.05$) increased the methane headspace concentration up to 16% for Y1 and 14% for Y2 (Table 8). A new study found that not only methanogens can produce methane, but all other non-methanogenic cells can produce methane (Ernst et al., 2022). In the study, they found that the fungi *S. cerevisiae* and *A. niger* significantly produce methane, especially with the addition of Fe^{2+} (Ernst et al., 2022). This could also explain why Y1 had more methane production than Y2, as the substrate it grew in contained Fe^{2+} from the trace element (Table 1). Nonetheless, Y2 was grown in liquid R2A medium (Table 4). The liquid R2A medium decreased the methane concentration by up to 8% (Appendix 2), so it may be that the increase in methane headspace concentration by the fungi overlapped with the reduction of methane in the headspace by the medium. Hence, the increase in the methane headspace concentration was not apparent.

Significant growth of cells was observed in both Y1 and Y2 (Figure 8). Furthermore, the increase in OD600 values was not significantly different between isolates treated with methane and the untreated controls, indicating less possibility for correlation between methane concentration increase and biomass growth. For Y2, the increase in cell number was negatively correlated, which may mean they grow more cells when producing methane as a byproduct. Y2 was found to be either *Pichia sp.*, *Saccharomyces sp.*, or *S. silvae* (Table 7). Contrary to our findings, other studies have found strains belonging to *Pichia* (Rozanov et al., 2020) and *Saccharomyces* absorbing methanol as their carbon source (Wolf & Hanson, 1980). Previous studies also reported the variety of behaviour of *Saccharomyces* sp.; some found that it significantly reduced methane, had no effect, or increased methane (Gong et al., 2013; Ernst et al., 2022). This reason for behavioral diversity has been postulated to be due to strain characteristics, growth nutrients, and dose (Gong et al., 2013).

Remarkably, the five fungal isolates behaved oppositely when dead/inactivated, particularly for F1, Y1 and Y2. Their behaviors in reducing methane were significantly different (Table 9). For instance, Y1 reduced methane headspace concentration by up to 19%, Y2 had 11 percentage unit lower methane production than their live biomass, and F1 increased methane headspace concentration by up to 14% (Table 9). Currently, there is no explanation available in the literature that could allow for conclusions as to why this dead yeast (Y1) had more capacity to uptake methane than their live counterparts. As mentioned, only Liew & Schilling found that the dead *Graphium* sp. biomass uptook methane 83% more effectively than live biomass (Liew & Schilling, 2020). However, the results for F1 and F3 were opposite. F1 and F3 showed that their dead biomass was less effective at reducing methane concentration. Instead, they even increased methane headspace concentrations (Table 9). Similarly, Ernst et al. showed that dead fungi cells slightly contribute to methane production (Ernst et al., 2022), but the mechanism remains unclear. In addition, Y2 had approximately 11 percentage unit lower increase in methane headspace, which means they were a more active contributor to methane production when alive, which may indicate that they contributed to methane release and when they were dead, the mechanism to produce methane was also inactivated. No significant differences in methane change existed between isolates pre-treated with methane and those not pre-treated.

Additionally, of the two yeast cultures we included in our study, Y1 turned out to be a bacterium, which was not expected (Figure 4). However, since we did not find out the PCR and DNA analysis outcomes until much later in the investigation, we proceeded with Y1. The ability of the strain *Pseudomonas migulae* to grow on antibiotic media shows its capacity to withstand the used antibiotics, possibly due to the presence of antibiotic resistance genes in its genome (Huyan et al., 2020), or with the help of biofilm formation, thereby resisting and protecting the bacterium from antibiotics (Abebe, 2020; Luo et al., 2022).

The study we implemented has shown that several strains of living and dead fungi may have a distinct impact on methane release and capture. Our analysis has highlighted that different conditions (i.e. growth substrate/media and whether the fungi are alive or dead) resulted in variations in the capacity to uptake methane, implying that both the physiological state of the fungi and the environmental context might influence methane uptake capacity. However, the high standard deviation in our study suggested variations among the replicates (n = 3). One possible reason was due to a non-ideal syringe used to draw out gas samples from the bottles for the GC instrument. Unfortunately, these plastic syringes were not gas-tight, which might have caused cross-contamination of sample volume and skewed results. This became further apparent when we conducted a small, replicated follow-up experiment with F1 to measure its carbon dioxide formation. We found out that the pressure produced by the generated carbon dioxide through respiration was high, which may have influenced our results in the previous experiments, which did not take changes in pressure into account. We suggest new experiments with more replicates and utilizing gas-tight syringes in future studies to provide more accuracy.

5 Conclusion

Based on the findings of this study, we can infer the possible capacity of some filamentous fungi and yeast strains to affect methane concentrations. Although filamentous fungi 1, 2, and 3 were assigned to the same strain *Trichoderma hazianum*, they all exhibited different behaviours in this study. Different conditions (i.e. growth substrate and whether the fungi are alive/dead) resulted in different physical structures and absorption capacities. This result indicates that physiological and environmental stimuli may lead to different responses from the fungi. One could use more than one gene marker to gain more insight into the fungal taxonomy and further understand the differences observed in this study and whether these differences were due to the media and/or genetics. Such a study could shed light on the underlying genetic and biochemical mechanisms that drive these differences and provide valuable insight into the capacity of *T. hazianum* in any future strategies for understanding methane cycling in fungi and reducing methane emissions. We observed that the five studied isolates had different relationships between their cell growth and methane headspace concentration change, challenging previous studies. Interestingly, one of our dead yeast counterparts could decrease methane concentrations. A more profound knowledge of this mechanism of dead yeast taking up methane should be examined further to understand better their capacity and mechanism to decrease methane. This study also highlighted the importance of using a gas-tight syringe and adding more replicates to increase accuracy. Thoroughly this study lays the foundation for the diverse capacity of filamentous fungi and yeast to decrease and increase methane concentrations, which in turn will create a pathway for more in-depth research into methane cycling and methane mitigation strategies and the potential of some strains of fungi for use in bioremediation.

References

Abebe, G. M. (2020). The role of bacterial biofilm in antibiotic resistance and food contamination. *International Journal of Microbiology*, *2020*, 1–10. https://doi.org/10.1155/2020/1705814

Adelusi, O. A., Gbashi, S., Adebiyi, J. A., Makhuvele, R., Adebo, O. A., Aasa, A. O., Targuma, S., Kah, G., & Njobeh, P. B. (2022). Variability in metabolites produced by Talaromyces Pinophilus SPJ22 cultured on different substrates. *Fungal Biology and Biotechnology*, *9*(1). https://doi.org/10.1186/s40694-022-00145-8

Badr, O., Probert, S. D., & O'Callaghan, P. W. (1992). Methane: A greenhouse gas in the Earth's atmosphere. *Applied Energy*, *41*(2), 95–113. https://doi.org/10.1016/0306-2619(92)90039-E

Berry, A. E., Chiocchini, C., Selby, T., Sosio, M., & Wellington, E. M. H. (2003). Isolation of high molecular weight DNA from soil for cloning into BAC Vectors. *FEMS Microbiology Letters*, *223*(1), 15–20. https://doi.org/10.1016/s0378-1097(03)00248-9

Chen, M. M., Coelho, P. S., & Arnold, F. H. (2012). Utilizing terminal oxidants to achieve p450-catalyzed oxidation of methane. *Advanced Synthesis & Catalysis*, *354*(6), 964–968. https://doi.org/10.1002/adsc.201100833

Črešnar, B., & Petrič, Š. (2011). Cytochrome P450 enzymes in the fungal kingdom. *Biochimica et Biophysica Acta (BBA) - Proteins and Proteomics*, *1814*(1), 29–35. https://doi.org/10.1016/j.bbapap.2010.06.020

del Prado, A., Lindsay, B., & Tricarico, J. (2023). Retrospective and projected warming-equivalent emissions from global livestock and cattle calculated with an alternative climate metric denoted GWP*. *PLOS ONE*, *18*(10). https://doi.org/10.1371/journal.pone.0288341

EPA, E. protection agency. (2023). *Importance of Methane*. Global Methane Initiative. https://www.epa.gov/gmi/importance-methane

Ernst, L., Steinfeld, B., Barayeu, U., Klintzsch, T., Kurth, M., Grimm, D., Dick, T. P., Rebelein, J. G., Bischofs, I. B., & Keppler, F. (2022). Methane formation driven by reactive oxygen

species across all living organisms. *Nature*, *603*(7901), 482–487. https://doi.org/10.1038/s41586-022-04511-9

Fischer, S., & Gillis, J. (2021). How many markers are needed to robustly determine a cell's type? *iScience*, *24*(11), 103292. https://doi.org/10.1016/j.isci.2021.103292

Girard, M., Viens, P., Ramirez, A. A., Brzezinski, R., Buelna, G., & Heitz, M. (2012). Simultaneous treatment of methane and swine slurry by biofiltration. *Journal of Chemical Technology & Biotechnology*, *87*(5), 697–704. https://doi.org/10.1002/jctb.3692

Gong, Y. L., Liao, X. D., Liang, J. B., Jahromi, M. F., Wang, H., Cao, Z., & Wu, Y. B. (2013). Saccharomyces cerevisiae Live Cells Decreased In vitro Methane Production in Intestinal Content of Pigs. *Asian-Australasian Journal of Animal Sciences*, *26*(6), 856–863. https://doi.org/10.5713/ajas.2012.12663

Gong, Y. L., Liang, J. B., Jahromi, M. F., Wu, Y. B., Wright, A. G., & Liao, X. D. (2018). Mode of action of saccharomyces cerevisiae in enteric methane mitigation in Pigs. *Animal*, *12*(2), 239–245. https://doi.org/10.1017/s1751731117001732

Guerrero-Cruz, S., Vaksmaa, A., Horn, M. A., Niemann, H., Pijuan, M., & Ho, A. (2021). Methanotrophs: Discoveries, environmental relevance, and a perspective on current and future applications. *Frontiers in Microbiology*, *12*. https://doi.org/10.3389/fmicb.2021.678057

Harnack K, Spolaczyk R, Janke S A. Turbidity measurements (OD600) with absorption spectrometers. Biospektrum, 1999, Vol. 6, 503-504

Hinrichs, K.-U., Hayes, J. M., Sylva, S. P., Brewer, P. G., & DeLong, E. F. (1999). Methane-consuming archaebacteria in marine sediments. *Nature*, *398*(6730), 802–805. https://doi.org/10.1038/19751

Huyan, J., Tian, Z., Zhang, Y., Zhang, H., Shi, Y., Gillings, M. R., & Yang, M. (2020). Dynamics of class 1 integrons in aerobic biofilm reactors spiked with antibiotics. *Environment International*, *140*, 105816. https://doi.org/10.1016/j.envint.2020.105816

Jackson, R. B., Saunois, M., Bousquet, P., Canadell, J. G., Poulter, B., Stavert, A. R., Bergamaschi, P., Niwa, Y., Segers, A., & Tsuruta, A. (2020). Increasing anthropogenic methane emissions arise equally from agricultural and fossil fuel sources. *Environmental Research Letters*, *15*(7), 071002. https://doi.org/10.1088/1748-9326/ab9ed2

Janke, S. A., Fortnagel, P., Bergmann, R. Microbiological turbidimetry using standard photometers. Biospektrum, 1999; Vol. 6: 501-502.

Jensen, S., Priemé, A., & Bakken, L. (1998). Methanol improves methane uptake in starved methanotrophic microorganisms. *Applied and Environmental Microbiology*, *64*(3), 1143–1146. https://doi.org/10.1128/aem.64.3.1143-1146.1998

Lane, D.J. (1991) 16S/23S rRNA Sequencing. In: Stackebrandt, E. and Goodfellow, M., Eds., Nucleic Acid Techniques in Bacterial Systematic, John Wiley and Sons, New York, 115-175.

Lebrero, R., López, J. C., Lehtinen, I., Pérez, R., Quijano, G., & Muñoz, R. (2016). Exploring the potential of fungi for methane abatement: Performance evaluation of a fungal-bacterial biofilter. *Chemosphere*, *144*, 97–106. https://doi.org/10.1016/j.chemosphere.2015.08.017

Liew, F. J., & Schilling, J. S. (2020). High-efficiency methane capture by living fungi and dried fungal hyphae (necromass). *Journal of Environmental Quality*, *49*(6), 1467–1476. https://doi.org/10.1002/jeq2.20136

Luo, A., Wang, F., Sun, D., Liu, X., & Xin, B. (2022). Formation, development, and cross-species interactions in biofilms. *Frontiers in Microbiology*, *12*. https://doi.org/10.3389/fmicb.2021.757327

Lynas, M., Houlton, B. Z., & Perry, S. (2021). Greater than 99% consensus on human caused climate change in the peer-reviewed scientific literature. *Environmental Research Letters*, *16*(11), 114005. https://doi.org/10.1088/1748-9326/ac2966

López, J. C., Quijano, G., Souza, T. S., Estrada, J. M., Lebrero, R., & Muñoz, R. (2013). Biotechnologies for greenhouse gases (CH4, n2o, and CO2) abatement: State of the art and

Challenges. *Applied Microbiology and Biotechnology*, *97*(6), 2277–2303. https://doi.org/10.1007/s00253-013-4734-z

Montzka, S. A., Dlugokencky, E. J., & Butler, J. H. (2011). Non-CO2 greenhouse gases and climate change. *Nature*, *476*(7358), 43–50. https://doi.org/10.1038/nature10322

Morgulis, A., Coulouris, G., Raytselis, Y., Madden, T. L., Agarwala, R., & Schäffer, A. A. (2008). Database indexing for production megablast searches. *Bioinformatics*, *24*(16), 1757–1764. https://doi.org/10.1093/bioinformatics/btn322

Myers, J. A., Curtis, B. S., & Curtis, W. R. (2013). Improving accuracy of cell and chromophore concentration measurements using optical density. *BMC Biophysics*, *6*(1). https://doi.org/10.1186/2046-1682-6-4

Myhre, G., & Shindell, D. (2014). Anthropogenic and Natural Radiative Forcing. In *Climate Change 2013 – The Physical Science Basis* (pp. 659–740). Cambridge University Press. https://doi.org/10.1017/CBO9781107415324.018

Odds, F. C. (1991). Sabouraud('s) agar. *Medical Mycology*, *29*(6), 355–359. https://doi.org/10.1080/02681219180000581

Oliver, J. P., & Schilling, J. S. (2016). Capture of Methane by Fungi: Evidence from Laboratory-Scale Biofilter and Chromatographic Isotherm Studies. *Transactions of the ASABE*, *59*(6), 1791–1801. https://doi.org/10.13031/trans.59.11595

Oliver, J. P., & Schilling, J. S. (2018). Harnessing fungi to mitigate CH4 in natural and engineered systems. *Applied Microbiology and Biotechnology*, *102*(17), 7365–7375. https://doi.org/10.1007/s00253-018-9203-2

Patel, A. K., Singhania, R. R., Albarico, F. P. J. B., Pandey, A., Chen, C.-W., & Dong, C.-D. (2022). Organic wastes bioremediation and its changing prospects. *Science of The Total Environment*, *824*, 153889. https://doi.org/10.1016/j.scitotenv.2022.153889

Posit team (2022). RStudio: Integrated Development Environment for R. Posit Software, PBC, Boston, MA. URL http://www.posit.co/.

Prenafeta-Boldú, F. X., de Hoog, G. S., & Summerbell, R. C. (2018). Fungal communities in hydrocarbon degradation. *Microbial Communities Utilizing Hydrocarbons and Lipids: Members, Metagenomics and Ecophysiology*, 1–36. https://doi.org/10.1007/978-3-319-60063-5_8-2

Reasoner, D. J., & Geldreich, E. E. (1985). A new medium for the enumeration and subculture of bacteria from potable water. *Applied and Environmental Microbiology*, *49*(1), 1–7. https://doi.org/10.1128/aem.49.1.1-7.1985

Rozanov, A. S., Pershina, E. G., Bogacheva, N. V., Shlyakhtun, V., Sychev, A. A., & Peltek, S. E. (2020). Diversity and occurrence of methylotrophic yeasts used in genetic engineering. *Vavilov Journal of Genetics and Breeding*, *24*(2), 149–157. https://doi.org/10.18699/vj20.602

Sadasivam, B. Y., & Reddy, K. R. (2014). Landfill methane oxidation in soil and bio-based cover systems: a review. *Reviews in Environmental Science and Bio/Technology*, *13*(1), 79–107. https://doi.org/10.1007/s11157-013-9325-z

Söhngen, N. L. (1906). Über bakterien, welche methan als kohlenstoffnahrung und energiequelle gebrauchen. Zentrabl Bakteriol Parasitenk Infektionskr, 15, 513-517.

Tedersoo, L., Bahram, M., Põlme, S., Kõljalg, U., Yorou, N. S., Wijesundera, R., Ruiz, L. V., Vasco-Palacios, A. M., Thu, P. Q., Suija, A., Smith, M. E., Sharp, C., Saluveer, E., Saitta, A., Rosas, M., Riit, T., Ratkowsky, D., Pritsch, K., Põldmaa, K., … Abarenkov, K. (2014). Global diversity and geography of soil fungi. *Science*, *346*(6213). https://doi.org/10.1126/science.1256688

Tedersoo, L., & Anslan, S. (2019). Towards pacbio-based Pan-eukaryote metabarcoding using full-length its sequences. Environmental Microbiology Reports, 11(5), 659–668. https://doi.org/10.1111/1758-2229.12776

Trippe, K. M., Wolpert, T. J., Hyman, M. R., & Ciuffetti, L. M. (2014). RNAi silencing of a cytochrome P450 monoxygenase disrupts the ability of a filamentous fungus, Graphium sp.,

to grow on short-chain gaseous alkanes and ethers. *Biodegradation*, *25*(1), 137–151. https://doi.org/10.1007/s10532-013-9646-1

Turner, S., Pryer, K. M., Miao, V. P., & Palmer, J. D. (1999). Investigating deep phylogenetic relationships among cyanobacteria and plastids by small subunit rrna sequence analysis1. *Journal of Eukaryotic Microbiology*, *46*(4), 327–338. https://doi.org/10.1111/j.1550-7408.1999.tb04612.x

VanderMolen, K. M., Raja, H. A., El-Elimat, T., & Oberlies, N. H. (2013). Evaluation of culture media for the production of secondary metabolites in a natural products screening program. *AMB Express*, *3*(1). https://doi.org/10.1186/2191-0855-3-71

Vergara-Fernández, A., Morales, P., Scott, F., Guerrero, S., Yañez, L., Mau, S., & Aroca, G. (2019). Methane biodegradation and enhanced methane solubilization by the filamentous fungi Fusarium solani. *Chemosphere*, *226*, 24–35. https://doi.org/10.1016/j.chemosphere.2019.03.116

Whittenbury, R., Phillips, K. C., & Wilkinson, J. F. (1970). Enrichment, isolation and some properties of methane-utilizing bacteria. *Journal of General Microbiology*, *61*(2), 205–218. https://doi.org/10.1099/00221287-61-2-205

Wolf, H. J., & Hanson, R. S. (1979). Isolation and characterisation of methane-utilizing yeasts. *Journal of General Microbiology*, *114*(1), 187–194. https://doi.org/10.1099/00221287-114-1-187

Wolf, H. J., & Hanson, R. S. (1980). Identification of methane-utilizing yeasts. *FEMS Microbiology Letters*, *7*(2), 177–179. https://doi.org/10.1111/j.1574-6941.1980.tb01602.x

Wong, C. (2023). Earth just had its hottest year on record — climate change is to blame. *Nature*, *623*(7988), 674–675. https://doi.org/10.1038/d41586-023-03523-3

Zajic, J. E., Volesky, B., & Wellman, A. (1969). Growth of *Graphium* sp. on natural gas. *Canadian Journal of Microbiology*, *15*(10), 1231–1236. https://doi.org/10.1139/m69-222

Zhang, Z., Schwartz, S., Wagner, L., & Miller, W. (2000). A greedy algorithm for aligning DNA sequences. *Journal of Computational Biology*, *7*(1–2), 203–214. https://doi.org/10.1089/10665270050081478

List of used abbreviations and symbols

ANME: Anaerobic methanotrophic archaea

ANOVA: Analysis of variance

approx.: Approximately

CH_4: Methane

°C: Degrees Celsius

BSA: Bovine serum albumin

DES: DNA elution solution

DNA: Deoxyribonucleic acid

dNTP: Deoxynucleotide triphosphate

FID: Flame ionization detector

F1: Filamentous fungi 1

F2: Filamentous fungi 2

F3: Filamentous fungi 3

g: Grams

GC: Gas chromatography

GHG: Greenhouse gas

GTDB: Genome taxonomy database

GWP: Global warming potential

h: Hour

HCl: Hydrochloric acid

HSD: Honestly significant difference

ITS: Internal transcribed spacer

KNO_3: Potassium nitrate

l: Litre

m: Metre

mA: Milliampere

min: Minute

mm: Millimetre

mM: Millimolar

ml: Millilitre

µl: Microlitre

NaCl: Sodium chloride

NCBI: National Center for Biotechnology Information

NIOO: Nederlands Instituut Voor Ecologie

NMS: Nitrate mineral salts

OD600: Optical density 600 nm

PBS: Phosphate buffer saline

PCR: Polymerase chain reaction

ppm: Parts per million

PPS: Protein precipitate solution

psi: Pound per square inch

RCF: Relative centrifugal force

rRNA: Ribosomal ribonucleic acid

R2A: Reasoner's 2A agar

S.D.: Standard deviation

SDA: Saboraud-4% Dextrose agar

SEWS-M: Salt ethanol wash

TAE: Tris-acetate-EDTA

U.S.: United States

UV: Ultraviolet

v: Volume

x g: (multiplies) Gravity

Y1: Yeast 1

Y2: Yeast 2

Y3: Yeast 3

$REE_2(CO_3)_3xH_2O$: Lanthanites

Na_2EDTA: Disodium ethylenediaminetetraacetate

$FeSO_4$ x $7H_2O$: Iron(II) sulfate heptahydrate

$ZnSO_4$ x $7H_2O$: Zinc sulfate heptahydrate

$MnCl_2$ x $4H_2O$: Manganese(II) chloride tetrahydrate

$CoCl_2$ x $6H_2O$: Cobalt(II) chloride hexahydrate

$CuCl_2$ x $2H_2O$: Copper(II) chloride dihydrate

$NiCl_2$ x $6H_2O$: Nickel(II) chloride hexahydrate

Na_2MoO_4 x $2H_2O$: Sodium molybdate dihydrate

Appendix

Appendix 1. Calibration curve for methane percentage calculation.

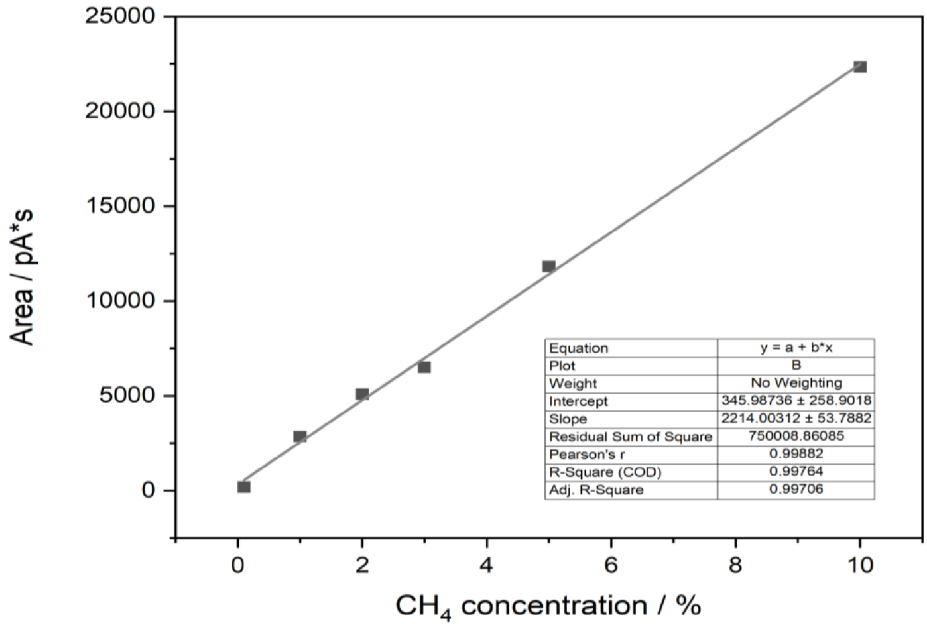

Appendix 2. Means (±standard deviation) of change in methane headspace (%) of four media used by the five fungi isolates (n=3 per media type) during the experiment.

Media	Change in methane headspace (%; Mean ± S.D.)
Solid SDA	-5.76 ± 0.38
Solid R2A	-9.93 ± 6.43
Liquid R2A	-7.70 ± 6.09
Liquid NMS	+5.06 ± 1.30

Appendix 3. Changes in methane headspace concentration (%) during the experiment **(a)** solid SDA media, **(b)** solid R2A media, **(c)** liquid NMS media, and **(d)** liquid R2A media (n=3, per media control). Points on day 1 and day 7 and 14 represent the initial and final methane headspace concentration, respectively. For SDA media, there were only two replicates because the other one leaked.